Journal of Ethnopharmacology 129 (2010) 335–343

Contents lists available at ScienceDirect

Journal of Ethnopharmacology

journal homepage: www.elsevier.com/locate/jethpharm

# Tetramethylpyrazine inhibits production of nitric oxide and inducible nitric oxide synthase in lipopolysaccharide-induced N9 microglial cells through blockade of MAPK and PI3K/Akt signaling pathways, and suppression of intracellular reactive oxygen species

Hong-Tao Liu[a], Yu-Guang Du[b], Jun-Lin He[c], Wen-Juan Chen[a], Wen-Ming Li[a], Zhu Yang[a], Ying-Xiong Wang[a], Chao Yu[a,*]

[a] Institute of Life Sciences, Chongqing Medical University, Chongqing 400016, China
[b] Dalian Institute of Chemical Physics, Chinese Academy of Sciences, Dalian 116023, China
[c] School of Public Health, Chongqing Medical University, Chongqing 400016, China

ARTICLE INFO

*Article history:*
Received 5 December 2009
Received in revised form 8 March 2010
Accepted 29 March 2010
Available online 3 April 2010

*Keywords:*
Tetramethylpyrazine
Inflammation
Inducible nitric oxide synthase
Microglial cell
Mitogen-activated protein kinase
PI3-kinase

ABSTRACT

*Aim of the study:* To determine the inhibitory effect of tetramethylpyrazine (TMP) on lipopolysaccharide (LPS)-induced over-production of nitric oxide (NO) and inducible nitric oxide synthase (iNOS) in N9 microglial cells.
*Materials and methods:* N9 cells were pretreated with vehicle or TMP and then exposed to LPS for the time indicated. Cell viability was determined by methylthiazoyltetrazolium (MTT) assay. Nitrite assay was performed by Griess reaction. Expression of iNOS mRNA was examined by RT-PCR. Protein levels of iNOS, p38 mitogen-activated protein kinase (MAPK), ERK1/2, JNK, phosphatidylinositol 3-kinase (PI3K) and Akt were determined by western blot analysis. Formation of reactive oxygen species (ROS) was evaluated by fluorescence image system.
*Results:* TMP inhibited LPS-induced over-production of NO and iNOS in N9 cells. TMP also inhibited the NF-κB translocation from cytoplasm into nucleus of N9 cells. In addition, TMP showed blocking effect on the phosphorylation of p38 MAPK, ERK1/2, JNK and Akt, but not PI3K. Further, TMP suppressed the formation of intracellular ROS in LPS-induced N9 cells.
*Conclusions:* TMP inhibited production of NO and iNOS in LPS-induced N9 cells through blocking MAPK and PI3K/Akt activation and suppressing ROS production.


## 1. Introduction

Microglial cells, functionally equivalent to peripheral macrophages in central nervous system, play a critical role in the pathogenesis of neurodegenerative diseases such as Parkinson's disease, Alzheimer's disease, HIV dementia and multiple sclerosis (Block et al., 2007). Upon activation, microglial cells will initiate the secretion of neurotoxic cytokines including tumor necrosis factor-α (TNF-α), interleukin-6 (IL-6), reactive oxygen species (ROS) and nitric products (Ma et al., 2009), which subsequently result in the occurrence of associated neurological diseases. Lipopolysaccharide (LPS), the major portion of outer membrane of gram-negative bacteria, is regarded as a main risk factor responsible for microglial cell activation (Qin et al., 2004; Bi et al., 2005; Zhu et al., 2008). Among LPS-induced inflammation reactions, the over-production of nitric oxide (NO) generated by inducible NO synthase (iNOS) has been paid more attention for its substantial contribution to microglial dysfunction. As a recognized marker of pro-inflammatory responses, the strong release of NO may trigger a series of inflammatory cascades in activated microglial cells (Stoll and Jander, 1999). Further, molecular mechanisms of LPS-induced NO and iNOS production in microglial cells are partly identified to be due to the activation of mitogen-activated protein kinase (MAPK) and phosphatidylinositol 3-kinase (PI3K)-Akt signaling pathways (Bhat and Fan, 2002; Kim et al., 2004). Therefore, blockade of these pro-inflammatory pathways followed by down-regulation of NO and iNOS levels in microglial cells may be an attractive therapeutic strategy against neurodegenerative diseases.

Tetramethylpyrazine (TMP) is a biologically active ingredient purified from the rhizome of *Ligusticum wallichi* (called chuanqiong in Chinese). For many years, TMP has been widely used in

* Corresponding author at: Box 174#, Institute of Life Sciences, Chongqing Medical University, 1 Yi Xue Yuan Road, Chongqing 400016, China. Tel.: +86 23 68485589; fax: +86 23 68486294.
*E-mail addresses:* yuchaom@163.com, paperyu@126.com (C. Yu).

0378-8741/$ – see front matter © 2010 Elsevier Ireland Ltd. All rights reserved.
doi:10.1016/j.jep.2010.03.037

China as one of the traditional Chinese medicines for its preventive effect on oxidative stress, myocardial injury, renal toxicity and hepatocellular injury, etc. (Liu et al., 2002; So et al., 2002; Zhou et al., 2004). In addition, recent studies *in vivo* and *in vitro* suggest that TMP protects central nervous system from injuries challenged by exogenous stimuli. For example, systemic administration of TMP significantly blocked neuronal degeneration in brains of rats (Tan, 2009). TMP might provide neuroprotection against ischemic brain injury in rats through suppression of inflammatory reaction (Kao et al., 2006). Moreover, TMP inhibited glioma activity and protected neurons against glioma-induced excitotoxicity (Fu et al., 2008). Nonetheless, no studies have provided direct evidence of TMP-mediated inhibitory effect on the overproduction of NO and iNOS in activated microglial cells, which may be important for further application of TMP against neuronal diseases.

In this study, we investigated the inhibitory effect of TMP on LPS-induced production of NO and iNOS in N9 microglial cells. We assessed TMP-mediated inhibition of NO secretion as well as suppression of iNOS at transcription and translation levels. To explore the underlying mechanisms by which TMP inhibited NO and iNOS production in LPS-induced N9 cells, the roles of signaling molecules including nuclear factor κB (NF-κB), MAPKs and PI3K/Akt were evaluated, and the scavenging effect of TMP on intracellular ROS was also determined.

## 2. Materials and methods

### 2.1. Chemicals and reagents

TMP (purity > 98%), 3-(4,5-dimethylthiazol-2-yl)-2,5-diphenyltetrazolium bromide (MTT), LPS from *Escherichia coli* and 2′,7′-dichlorofluorescein diacetate (DCFH-DA) were obtained from Sigma (St. Louis, MO, USA). P38 MAPK inhibitor (SB203580), ERK1/2 inhibitor (PD98059) and c-Jun N-terminal kinase (c-JNK) inhibitor (SP600125) were purchased from Invitrogen Corporation (Carlsbad, CA, USA). PI3K inhibitor (LY294002) was obtained from Beyotime Institute of Biotechnology (Jiangsu, China). Polyclonal rabbit or mouse antibodies against p38 MAPK, phospho-p38 (p-p38) MAPK, ERK1/2, phospho-ERK1/2 (p-ERK1/2), JNK, phospho-JNK, Akt (Thr 308), phospho-Akt (Thr 308), PI3K, phospho-PI3K, iNOS, β-actin and horseradish peroxidase (HRP)-conjugated goat anti-rabbit or mouse IgG were purchased from Santa Cruz Biotechnology (Santa Cruz, CA, USA). Polyclonal rabbit antibody against NF-κB was obtained from Beyotime Institute of Biotechnology (Jiangsu, China). Iscove's modified dulbecco's medium (IMDM) and fetal bovine serum (FBS) were purchased from Gibco (Grand Island, NY, USA).

### 2.2. Cell culture and drug treatment

The murine microglial cell line N9 was a kind gift from Professor Yun Bai (the 3rd Military Medical University, Chongqing, China). Cells were cultured in IMDM supplemented with 10% FBS, 0.5% β-mercaptoethanol, 1% glutamine, 100 units/ml penicillin, 100 units/ml streptomycin and 5 units/ml heparin in a humidified atmosphere of 5% $CO_2$ and 95% $O_2$ at 37 °C.

For most experiments, N9 cells grown to sub-confluence were pretreated with vehicle or TMP (25–100 μg/ml) for 4–24 h. After pretreatment, cells were challenged with LPS (1 μg/ml) in presence or absence of TMP for the time indicated and then subjected to further analysis. TMP was dissolved in dimethylformamide (DMSO, <0.1%), which showed no deleterious effect on the viability of N9 cells in preliminary studies.

### 2.3. Determination of cell viability

Cell viability was determined by the conversion of MTT to formazan (Tarozzi et al., 2007). In brief, N9 cells were seeded in 96-well microtiter plates at a concentration of $7.5 \times 10^3$ cells/well and treated with TMP and/or LPS for the indicated time periods. After treatment, culture medium was removed and the cells were incubated with MTT (5 mg/ml) for 3 h at 37 °C. The formazan blue, which formed in cells, was solubilized in 100 μl of DMSO. The optical density was measured at 490 nm using a Sunrise Remote Microplate Reader (Grodlg, Austria). The viability of N9 cells in each well was presented as percentage of the control level (untreated).

### 2.4. Nitrate assay

NO production from activated N9 cells was determined based on the accumulation of nitrite ($NO^{2-}$), a stable metabolite of NO and molecular oxygen (Nizamutdinova et al., 2008). After treatment with TMP and/or LPS, the culture medium in N9 cells was harvested. An aliquot of the culture supernatant (50 μl) was mixed with an equal volume of Griess reagent (1% sulfanilamide and 0.1% N-naphthylethyl-ethylenediamine dihydrochloride in 5% phosphoric acid) for 15 min at room temperature. The optical density was measured at 540 nm using a Sunrise Remote Microplate Reader (Grodlg, Austria). Nitrite concentration was calculated with reference to a standard curve of sodium nitrite generated by known concentrations.

### 2.5. Measurement of NO scavenging activity

The direct scavenging effect of TMP on NO was measured according to the reported method with some modification (Marcocci et al., 1994). Briefly, 0.2 ml of sodium nitroprusside (SNP) (10 mM) was incubated with 1.8 ml of phosphate-buffered saline (PBS) or different concentrations of TMP in light at 25 °C. After incubation for 2 h, the supernatant was collected and nitrite levels were determined by Griess reaction as described in Section 2.4.

### 2.6. Reverse transcription-polymerase chain reaction (RT-PCR)

For RT-PCR, total RNA was extracted using cold TRIZOL reagent (Takara, Dalian, China) according to the manufacturer's protocol. Reverse transcription was carried out at 42 °C for 1 h in a reaction mixture containing 1 μg of total RNA, 25 pmol of oligo-dT primer, 10 nmol of dNTP mixture, 20 units of RNase inhibitor and 2.5 units of AMV reverse transcriptase (Bioer, Hangzhou, China). PCR was performed using the prepared cDNA as templates, with following cycle parameters: 4 min at 94 °C for initial denaturation; 30 cycles × 30 s at 94 °C, 45 s at 53 °C, and 45 s at 72 °C for iNOS; 30 cycles × 30 s at 94 °C, 30 s at 54 °C, and 30 s at 72 °C for β-actin. The primer sequences were as follows: 5′-TGG AGC GAG TTG TGG ATT GTC-3′ (sense), 5′-CCC TTT GTG CTG GGA GTC AT-3′ (anti-sense) for iNOS (650 bp); 5′-GAT GGT GGG AAT GGG TCA GA-3′ (sense), 5′-GGA GAG CAT AGC CCT CGT AGA T-3′ (anti-sense) for β-actin (386 bp). The PCR products were visualized by electrophoresis in 1.5% agarose gel containing 1% GoldView™. Band intensity was analyzed with ImageJ system (NIH, USA).

### 2.7. Preparation of cell lysates

Cytoplasmic and nuclear extracts were prepared using Nuclear and Cytoplasmic Protein Extraction kit according to the manufacturer's instructions (Beyotime Institute of Biotechnology, Jiangsu, China). The experimental procedures were as followed: (1) after drug treatment, N9 cells were washed with ice-cold PBS twice, detached and collected; (2) after centrifugation at 1000 × *g* for

5 min at 4 °C, the supernatant was discarded and the cells were fully resuspended in 200 μl of cytoplasmic protein extraction reagent (CPER) A; (3) the cell suspension was violently vortexed for 5 s and incubated on ice for 10 min; (4) 10 μl of CPER B was added to each tube followed by vigorous vortex for 5 s and the incubation on ice for 1 min was performed; (5) after vigorous vortex for 5 s, the cell lysate was centrifuged at 16,000 × *g* for 5 min at 4 °C and the supernatant was aliquoted for cytoplasmic proteins; (6) the insoluble cell pellets were resuspended in 50 μl of nuclear protein extraction reagent and successively vortexed for 15 s every 2 min for a total of 30 min on ice; (7) the supernatant fraction containing nuclear proteins was collected by centrifugation at 16,000 × *g* for 10 min at 4 °C.

For isolation of total cell extracts, cells were lysed in 200 μl of RIPA lysis buffer (50 mM Tris with pH 7.4, 150 mM NaCl, 1% Triton X-100, 1% sodium deoxycholate, 0.1% SDS and 0.05 mM EDTA). The cell lysate was incubated on ice for 30 min and mixed with a vortex every 5 min. After that, the lysate was centrifuged at 12,000 × *g* for 15 min at 4 °C and the supernatant was collected as total cell extracts. Protein concentration was quantified by the Bicinchoninic Acid Protein Assay kit (Biomed Biotech Co., Ltd., Beijing, China). All samples were stocked at −80 °C until further analysis.

### 2.8. Western blot analysis

Levels of target proteins including iNOS, NF-κB, p-p38, p-38, p-ERK1/2, ERK1/2, p-JNK, JNK, p-PI3K, PI3K, p-Akt, Akt and β-actin were determined by Western blot analysis using the respective antibodies stated above. Briefly, cell lysate was boiled in 5 × loading buffer (125 mM Tris·HCl, pH 6.8, 10% SDS, 8% dithiothreitol, 50% glycerol and 0.5% bromchlorphenol blue) for 10 min. Equal amount of protein samples (50 μg) was separated by 6–12% SDS-polyacrylamide gel and transferred to polyvinylidene fluoride membranes. The membranes were blocked with 5% skim milk in PBS with 0.1% Tween 20 (PBST) for 1 h, and incubated with primary antibodies overnight at 4 °C. After washing with PBST, HRP-conjugated secondary antibodies were applied and the blots were developed using enhanced chemiluminescence reagents (ECL). Densitometric analysis was performed with the use of PDI Imageware System (Bio-Rad, Hercules, CA, USA).

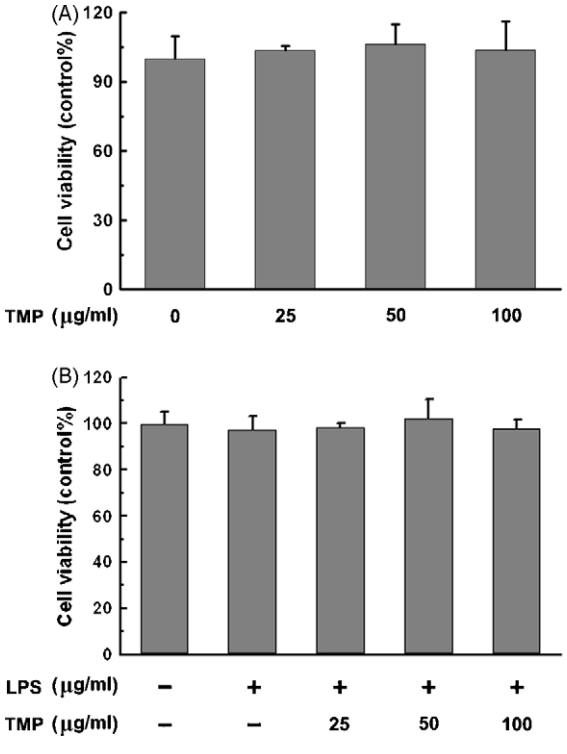


**Fig. 1.** Effect of TMP and/or LPS treatment on N9 cell viability. (A) Cells were treated with vehicle or TMP (25–100 μg/ml) for 24 h. (B) Cells were pretreated with vehicle or TMP (25–100 μg/ml) for 4 h and then exposed to LPS (1 μg/ml) for 20 h. After treatment, cell viability was determined by MTT analysis ($n = 5$) as described in Section 2. Data are expressed as means ± SD.

### 2.9. Intracellular ROS measurement

For measurement of the intracellular ROS levels, N9 cells were incubated with 20 μM DCFH-DA in culture medium at 37 °C for 1 h. After incubation, cells were washed with PBS, and fluorescence images of random fields were captured using a Leica DMRX microscope (Wetzlar, Germany). Fluorescent intensity of each picked image was measured with Image-Pro Plus 6.0 software (Media Cybernetics, USA).

### 2.10. Statistics

Statistical evaluation was carried out using SPSS 10.0 package (SPSS Inc., Chicago, IL, USA). Data were expressed as mean ± SD of 3–5 independent experiments. Statistical differences between groups were determined using one-way ANOVA and Student's *t*-test followed by a Bonferroni correction. Values of $P < 0.05$ were considered to be statistically significant.

## 3. Results

### 3.1. TMP and/or LPS treatment show no inhibitory effect on N9 cell viability

Effect of TMP on N9 cell viability was evaluated by MTT assay. Results show that TMP incubation alone for 24 h at concentrations of 25, 50 and 100 μg/ml had no effect on the viability of N9 cells (Fig. 1A). Additionally, when cells were pretreated with TMP (25, 50 and 100 μg/ml) for 4 h before exposed to LPS (1 μg/ml) for 20 h, no significant difference in cell viability was found in comparison with the vehicle-treated group (Fig. 1B). Thus, for this study, we used TMP at concentrations of 25–100 μg/ml, which caused no cytotoxicity for the following experiments of anti-inflammatory property and action mechanisms in LPS-induced N9 cells.

### 3.2. TMP shows no scavenging effect on NO production in SNP solution, but suppresses LPS-induced NO production in N9 cells

As an exogenous NO donator, SNP can lead to the generation of nitrate under light irradiation. Results in Fig. 2A indicate that, after incubation for 2 h, SNP (10 mM) generated quite a large amount of nitrite (9.8 ± 0.4 μM, $P < 0.01$, *vs* the blank group), and this high level of nitrite was not significantly decreased by the presence of TMP (25–100 μg/ml). It is presumed that TMP has no direct scavenging effect on NO production in SNP solution.

The suppression of NO production in LPS-induced N9 cells was measured by Griess reaction. As shown in Fig. 2B, the NO level in vehicle-treated cells was minimal (0.2 ± 0.1 μM) and a pronounced increase was observed after LPS exposure (1 μg/ml) for 20 h (5.4 ± 0.4 μM, $P < 0.01$, *vs* the vehicle-treated group). On the contrary, pretreatment with TMP for 4 h dose-dependently suppressed LPS-induced NO production in N9 cells (25 μg/ml, 3.8 ± 0.6 μM, $P < 0.05$; 50 μg/ml, 3.1 ± 0.4 μM, $P < 0.01$; 100 μg/ml, 1.8 ± 0.3 μM, $P < 0.01$, *vs* the LPS-treated group).

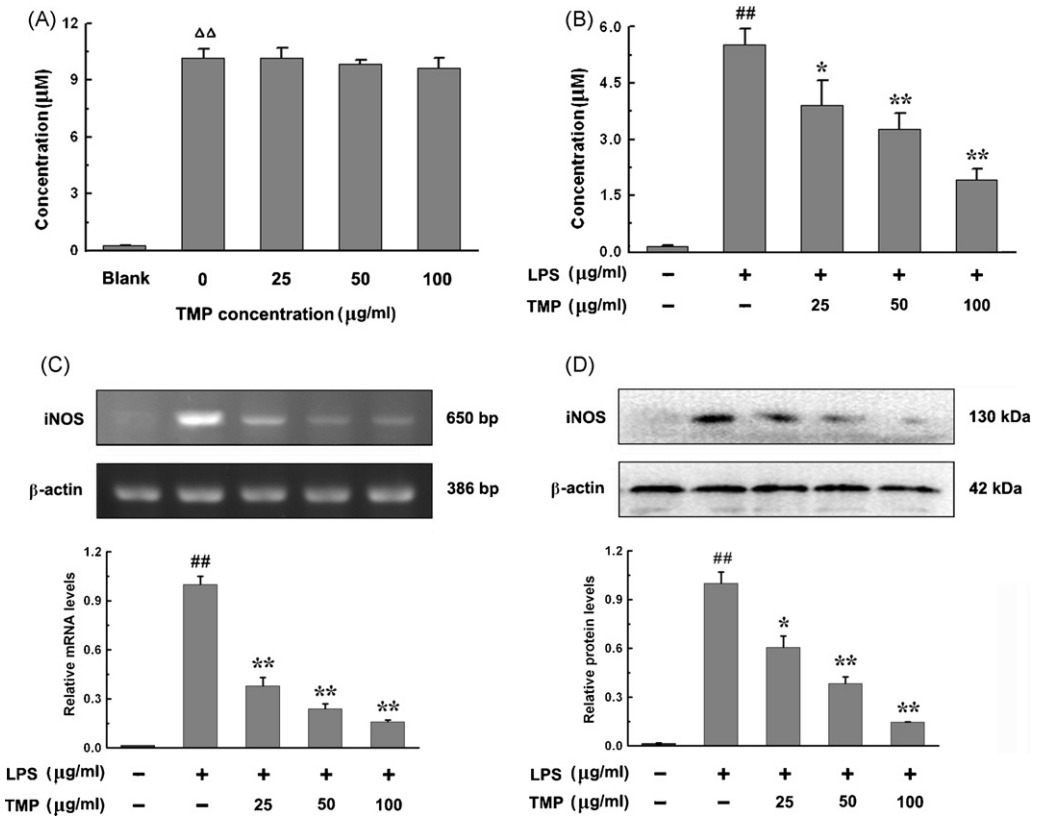


**Fig. 2.** Effect of TMP on NO and iNOS levels in SNP solution or in LPS-induced N9 cells. (A) SNP solution (10 mM) was incubated with PBS or TMP (25–100 μg/ml) in light at 25 °C for 2 h. After incubation, nitrate levels were measured by Griess reaction as described in Section 2. (B) Cells were pretreated with TMP (25–100 μg/ml) for 4 h and then exposed to LPS (1 μg/ml) for 20 h. After treatment, nitrite levels in culture medium were measured by Griess reaction as described in Section 2. (C) Cells were pretreated with TMP (25–100 μg/ml) for 18 h and then exposed to LPS (1 μg/ml) for 6 h. After treatment, the mRNA level of iNOS was determined by RT-PCR analysis as described in Section 2. (C) Cells were pretreated with TMP (25–100 μg/ml) for 4 h and then exposed to LPS (1 μg/ml) for 20 h. After treatment, the protein level of iNOS was determined by Western blot analysis as described in Section 2. Data are representative of three experiments (means ± SD). $^{\Delta\Delta}P < 0.01$ compared to the blank group (PBS alone); $^{\#\#}P < 0.01$ compared to the vehicle-treated group; $^{*}P < 0.05$, $^{**}P < 0.01$ compared to the LPS-treated group.

### 3.3. TMP inhibits LPS-induced iNOS expression at transcription and translation levels in N9 cells

To study the effect of TMP on LPS-induced over-expression of iNOS mRNA, N9 cells were pretreated with different concentrations of TMP (25–100 μg/ml) for 18 h and then exposed to LPS (1 μg/ml) for 6 h. Prior to LPS stimulation, the cells produced undetectable mRNA level of iNOS by RT-PCR analysis (Fig. 2C). However, LPS challenge led to a high expression of iNOS mRNA, and this over-expression was inhibited by TMP pretreatment (25 μg/ml, 38.4 ± 1.9%, $P < 0.01$; 50 μg/ml, 23.7 ± 3.3%, $P < 0.01$; 100 μg/ml, 16.5 ± 2.0%, $P < 0.01$, *vs* the LPS-treated group).

The inhibition of iNOS by TMP at protein level in LPS-induced N9 cells was also tested by Western blot analysis. As indicated in Fig. 2D, cells in the vehicle-treated group almost showed no protein expression of iNOS, which was remarkably induced by LPS (1 μg/ml) challenge for 20 h. TMP pretreatment for 4 h effectively alleviated LPS-induced iNOS production (25 μg/ml, 60.6 ± 7.3%, $P < 0.05$; 50 μg/ml, 38.5 ± 4.2%, $P < 0.01$; 100 μg/ml, 14.6 ± 0.4%, $P < 0.01$, *vs* the LPS-treated group), suggesting a similar inhibitory effect as revealed in Fig. 2C.

### 3.4. TMP shows blocking effect on LPS-induced NF-κB translocation into nucleus of N9 cells

Because increased expression of iNOS is known to be associated with the activation of NF-κB (Mukaida et al., 1996), we assessed the inhibitory effect of TMP on LPS-induced NF-κB translocation from cytoplasm into nucleus of N9 cells. Results in Fig. 3 suggest that LPS (1 μg/ml) challenge for 6 h promoted the NF-κB translocation into nucleus of N9 cells as indicated by a markedly changed protein level of NF-κB, which was decreased in cytoplasm (53.6 ± 4.8%, $P < 0.01$) and increased in nucleus (147.6 ± 13.3, $P < 0.01$), compared to the vehicle-treated group. In contrast, TMP pretreatment for 18 h evidently directed the up-regulation of cytoplasmic NF-κB p65 protein levels (25 μg/ml, 152.4 ± 19.7%, $P < 0.05$; 50 μg/ml, 166.3 ± 13.3%, $P < 0.01$; 100 μg/ml, 220.7 ± 13.2%, $P < 0.01$, *vs* the LPS-treated group) and down-regulation of nuclear NF-κB p65 protein levels (25 μg/ml, 56.5 ± 7.4%, $P < 0.01$; 50 μg/ml, 43.1 ± 3.4%, $P < 0.01$; 100 μg/ml, 41.4 ± 2.5%, $P < 0.01$, *vs* the LPS-treated group), indicating that TMP inhibited LPS-induced NF-κB activation in N9 cells.

### 3.5. TMP inhibits LPS-induced phosphorylation of MAPKs including p38 MAPK, ERK1/2 and JNK in N9 cells

To clarify whether TMP inhibits LPS-induced MAPK activation, N9 cells were pretreated with TMP (25–100 μg/ml) for 24 h and then exposed to LPS (1 μg/ml) for 30 min. As shown in Fig. 4, all of the three MAPK members including p38 MAPK, ERK1/2 and JNK were highly phosphorylated in N9 cells treated by LPS alone (272.1 ± 29.2%, $P < 0.01$; 207.2 ± 18.6%, $P < 0.01$; 489.6 ± 78.4%, $P < 0.01$, respectively) as compared to the vehicle-treated group. On the other hand, LPS-induced p38 phosphorylation was inhibited by TMP pretreatment in a dose-dependent manner (25 μg/ml, 63.4 ± 6.3%, $P < 0.01$; 50 μg/ml, 44.7 ± 3.4%, $P < 0.01$; 100 μg/ml, 46.2 ± 5.8%, $P < 0.01$, *vs* the LPS-treated group). Also, the elevated phosphorylation of ERK1/2 and JNK were reversed by TMP at higher concentrations (50–100 μg/ml), and the relative phosphorylation

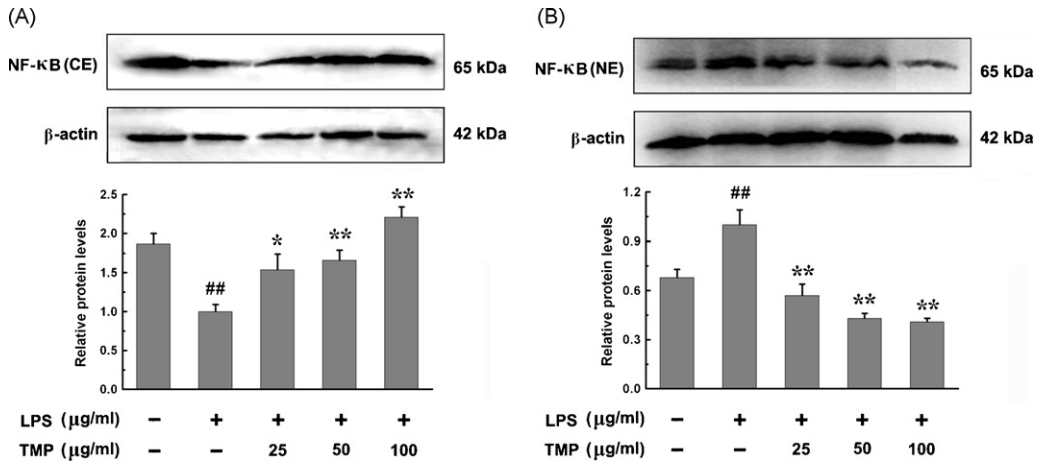


**Fig. 3.** Effect of TMP on nuclear translocation of NF-κB in LPS-induced N9 cells. CE: cytoplasmic extracts; NE: nuclear extracts. (A) Relative protein levels of NF-κB in cytoplasm of N9 cells; (B) relative protein levels of NF-κB in nucleus of N9 cells. Cells were pretreated with TMP (25–100 μg/ml) for 18 h and then exposed to LPS (1 μg/ml) for 6 h. After treatment, nuclear and cytoplasmic fractions were analyzed for detection of NF-κB by Western blot analysis as described in Section 2. Data are representative of three experiments (means ± SD). $^{\#\#}P < 0.05$ compared to the vehicle-treated group; $^{*}P < 0.05$, $^{**}P < 0.01$ compared to the LPS-treated group.

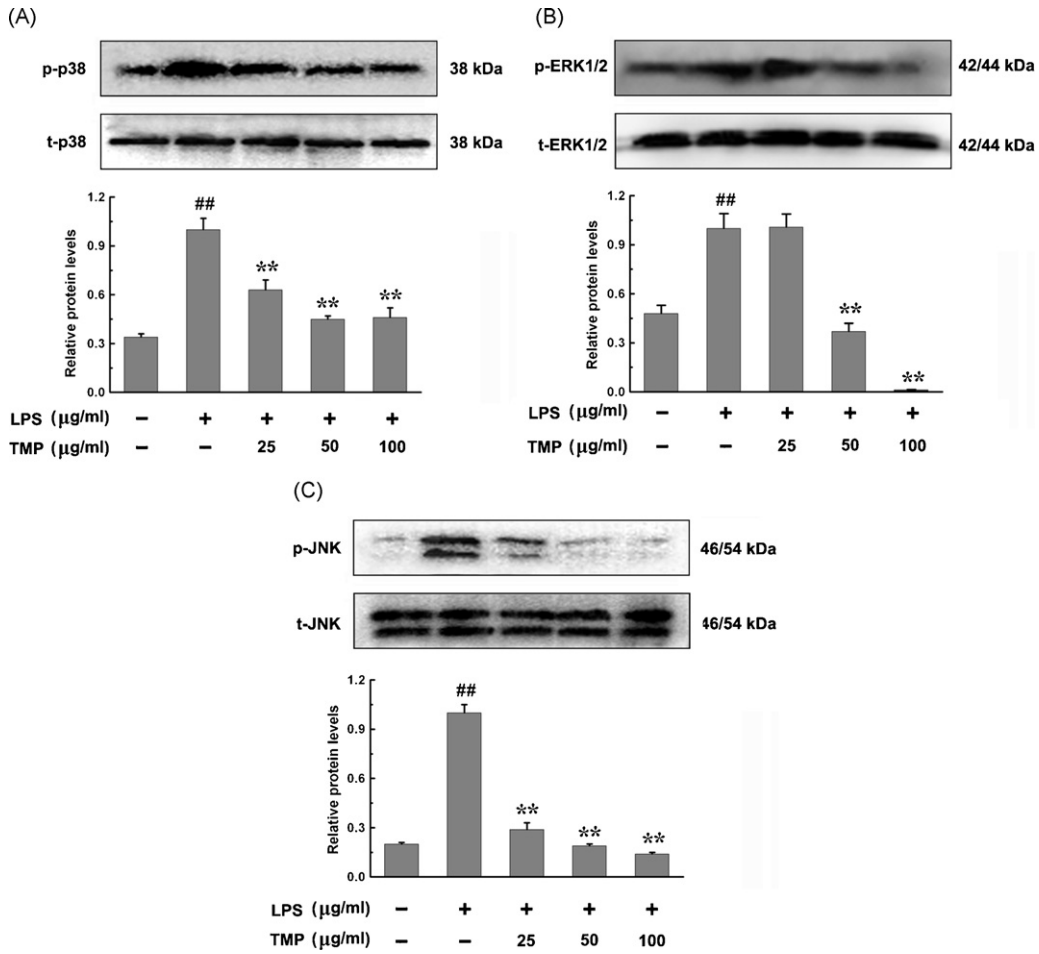


**Fig. 4.** Effect of TMP on LPS-induced phosphorylation of MAPKs including p38 MAPK (A), ERK1/2 (B) and JNK (C) in N9 cells. Cells were pretreated with TMP (25–100 μg/ml) for 24 h and then exposed to LPS (1 μg/ml) for 30 min. After treatment, total cell extract was prepared and the protein levels of phosphorylated p38 MAPK (p-p38), total p38 MAPK (t-p38), phosphorylated ERK1/2 (p-ERK1/2), total ERK1/2 (t-ERK1/2), phosphorylated JNK (p-JNK) and total JNK (t-JNK) were determined by Western blot analysis as described in Materials and methods. Data are representative of three experiments (means ± SD). $^{\#}P < 0.05$, $^{\#\#}P < 0.01$ compared to the vehicle-treated group; $^{**}P < 0.01$ compared to the LPS-treated group.

magnitudes of both MAPK members in TMP-pretreated cells were as follows: 50 μg/ml, 36.7 ± 4.8% for p-ERK and 18.9 ± 4.2% for p-JNK, $P < 0.01$; 100 μg/ml, 0.5 ± 0.1% for p-ERK and 14.3 ± 2.7% for p-JNK, $P < 0.01$, *vs* the LPS-treated group.

### 3.6. TMP shows inhibitory effect on LPS-induced phosphorylation of Akt, but not PI3K in N9 cells

Next, we determined the effect of TMP on PI3K/Akt signaling pathway, which was confirmed to be implicated in regulation of inflammatory cytokines in microglial cells (Kim et al., 2004). Results in Fig. 5 show that LPS (1 μg/ml) exposure for 30 min induced a rapid increase in the protein levels of both p-PI3K and p-Akt in N9 cells (246.6 ± 29.6%, $P < 0.01$; 142.4 ± 10.0%, $P < 0.05$, respectively, *vs* the vehicle-treated group). After pretreatment with TMP at concentrations of 25, 50 and 100 μg/ml for 24 h, the phosphorylated Akt level was reduced to 66.3 ± 3.3% ($P < 0.05$), 20.0 ± 1.6% ($P < 0.01$) and 25.6 ± 3.1% ($P < 0.01$) of the LPS-treated group, respectively. In addition, TMP pretreatment failed to alter LPS-induced p-PI3K level. These results indicate that TMP may inhibit the Akt activation, but not PI3K in LPS-induced N9 cells.

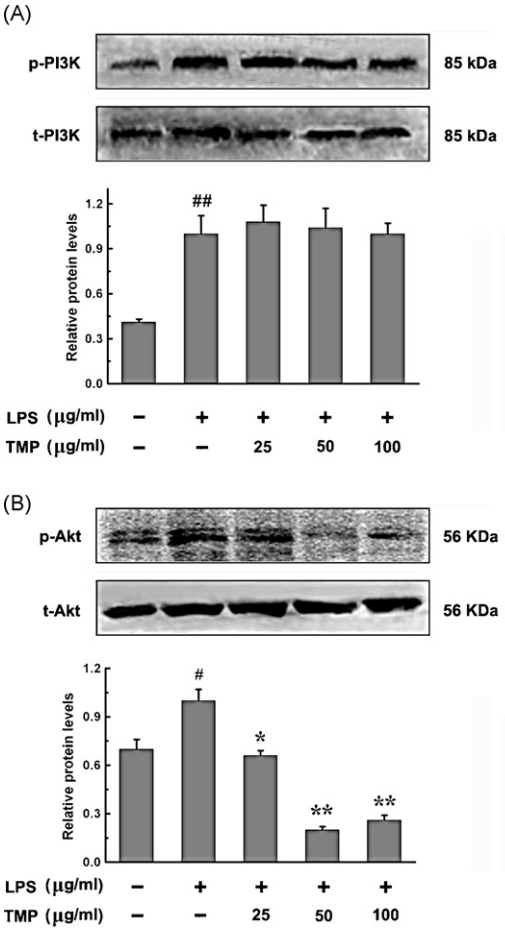


**Fig. 5.** Effect of TMP on LPS-induced phosphorylation of PI3K (A) and Akt (B) in N9 cells. Cells were pretreated with TMP (25–100 μg/ml) for 24 h and then exposed to LPS (1 μg/ml) for 30 min. After treatment, total cell extract was prepared and the protein levels of phosphorylated PI3K (p-PI3K), total PI3K (t-PI3K), phosphorylated Akt (p-Akt), and total Akt (t-Akt) were determined by Western blot analysis as described in Materials and methods. Data are representative of three experiments (means ± SD). $^{\#}P < 0.05$, $^{\#\#}P < 0.01$ compared to the vehicle-treated group; $^{*}P < 0.05$, $^{**}P < 0.01$ compared to the LPS-treated group.

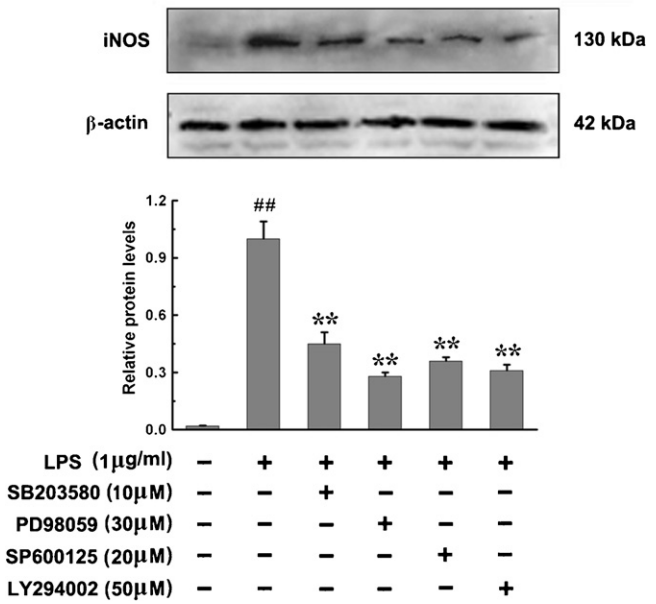


**Fig. 6.** Effects of p38 inhibitor, SB203580, ERK1/2 inhibitor, PD98059, JNK inhibitor, SP600125 and PI3K inhibitor, LY294002, on LPS-induced iNOS production in N9 cells. Cells were pretreated with SB203580 (10 μM), PD98059 (30 μM), SP600125 (20 μM) or LY294002 (50 μM) for 1 h and then exposed to LPS (1 μg/ml) for 20 h. After treatment, total cell extract was prepared and the protein level of iNOS was determined by Western blot analysis as described in Materials and methods. Data are representative of three experiments (means ± SD). $^{\#\#}P < 0.01$ compared to the vehicle-treated group; $^{**}P < 0.01$ compared to the LPS-treated group.

### 3.7. Inhibitors of p38 MAPK, ERK1/2, JNK and PI3K inhibit LPS-induced iNOS production in N9 cells

To verify whether MAPK and PI3K/Akt signaling pathways are involved in LPS-induced iNOS production, N9 cells were pretreated with p38 MAPK inhibitor, SB203580, ERK1/2 inhibitor, PD98059, JNK inhibitor, SP600125, or PI3K inhibitor, LY294002, for 1 h and then exposed to LPS (1 μg/ml) for 20 h. In keeping with our previous experiment, LPS challenge for 20 h induced a pronounced up-regulation of iNOS protein level in N9 cells (Fig. 6). By contrast, pretreatment with the specific inhibitors including SB203580 (10 μM), PD98059 (30 μM), SP600125 (20 μM), or LY294002 (50 μM) significantly inhibited LPS-induced over-production of iNOS, which was decreased to 45.4 ± 5.9% ($P < 0.01$), 28.1 ± 2.3 ($P < 0.01$), 36.3 ± 2.2% ($P < 0.01$) and 30.5 ± 3.4% ($P < 0.01$), respectively, compared to the LPS-treated group. No significant inhibition of iNOS was observed when N9 cells were incubated with SB203580, PD98059, SP600125 and LY294002 alone (data not shown).

### 3.8. TMP suppresses LPS-induced intracellular ROS formation in N9 cells

Once diffusion into cells, the non-fluorescent dye DCFH-DA is conversed into DCF, a fluorescent product, by intracellular esterases and oxidation occurs (Kilic et al., 2006). Therefore, enhanced oxidative stress within cells can be reflected by monitoring the increase in fluorescence. Accordingly, we examined whether TMP modulates LPS-induced intracellular ROS formation in N9 cells. Exposure of cells to LPS (1 μg/ml) for 20 h significantly increased the intracellular ROS level to 351.6 ± 14.1% of the vehicle-treated group ($P < 0.01$) (Fig. 7A and B). Such elevation of intracellular ROS was inhibited by pretreatment with TMP for 4 h in a dose-dependent manner (25 μg/ml, 71.9 ± 3.6%, $P < 0.05$; 50 μg/ml, 63.8 ± 7.0%, $P < 0.01$; 100 μg/ml, 44.3 ± 2.7%, $P < 0.01$, *vs* the LPS-treated group) (Fig. 7C and D).

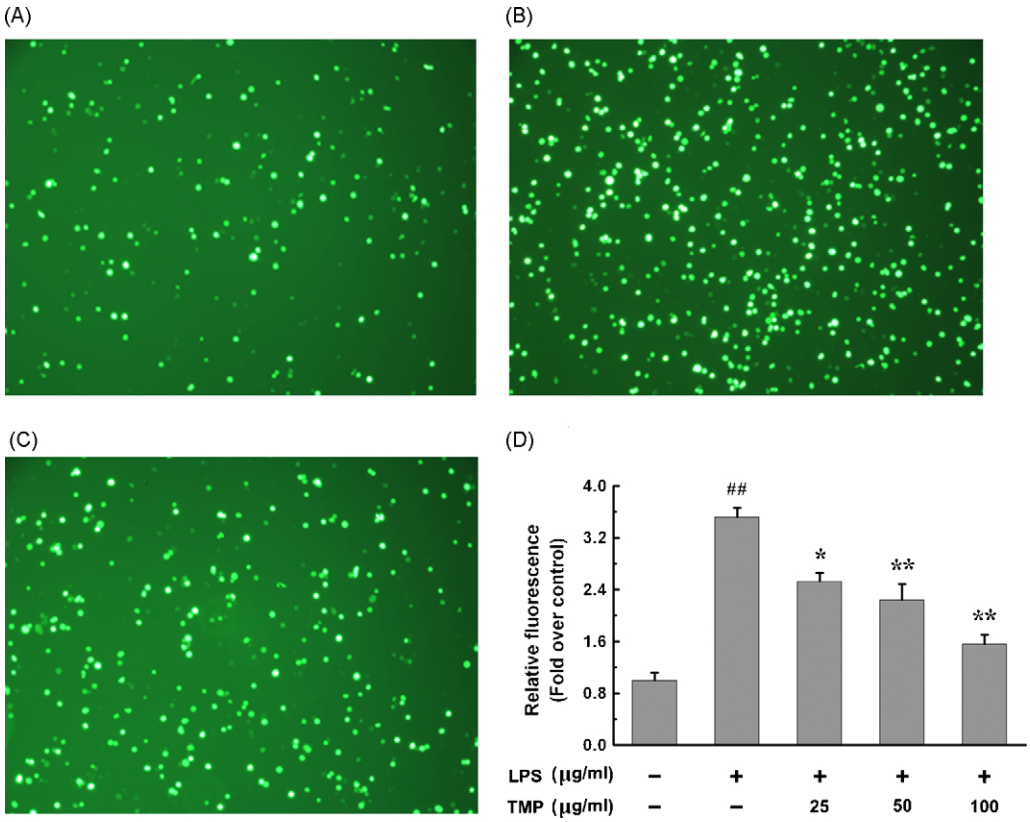


**Fig. 7.** Effect of TMP on LPS-induced intracellular ROS formation in N9 cells. Cells were pretreated with TMP (25–100 μg/ml) for 4 h and then exposed to LPS (1 μg/ml) for 20 h. After treatment, cells were washed with PBS and the fluorescence intensity was measured by flow cytometry as described in Materials and methods. A–C showed representative flow cytometric histograms of vehicle-treated cells, cells exposed to 1 μg/ml of LPS for 20 h and cells pretreated with 100 μg/ml of TMP for 4 h before exposed to 1 μg/ml of LPS for 20 h, respectively. Fig. 7D presented the fluorescent intensities of N9 cells treated with vehicle, TMP and/or LPS. Data are expressed as means ± SD ($n = 3$). $^{\#\#}P < 0.01$ compared to the vehicle-treated group; $^{*}P < 0.05$, $^{**}P < 0.01$ compared to the LPS-treated group.

## 4. Discussion

Microglial cells are vulnerable to infiltrating inflammatory mediators and can readily become activated by stimulation with LPS, β-amyloid, interferon (IFN)-γ or adenosine triphosphate (ATP) (Inoue, 2002; Bamberger et al., 2003; Pawate et al., 2004). Activated microglial cells migrate to the brain where they damage normal brain cells by secreting a number of pro-inflammatory and neurotoxic factors as above-mentioned (Wang et al., 2009). It seems that pharmacological interventions targeting the suppression of microglial cell activation may be a key step against neuro-inflammations. In recent reports, several anti-inflammatory agents like Fluvastatin, Ketamine and Resveratrol have displayed remarkable suppressive effects on the production of NO/iNOS and other inflammatory effectors in microglial cells (Bi et al., 2005; Xu et al., 2008; Chang et al., 2009). For the first time, we here demonstrate that TMP inhibits the NO/iNOS production in LPS-induced N9 cells through blockade of MAPK and PI3K/Akt signaling pathways.

NO is a highly reactive free radical and plays an important role in response to many physiological and pathological conditions (Moncada et al., 1991). While NO is beneficial as an intracellular messenger or modulator, the excessive production of NO synthesized by iNOS has been defined as a cytotoxic molecule in inflammation and endotoxemia (Brochu et al., 1999). Activated microglial cells are shown to kill neurons via NO from iNOS through inhibiting neuronal respiration (Bal-Price and Brown, 2001), and LPS has been documented to represent one of the most potent stimuli for iNOS production in microglial cells (Garrido et al., 2004). In previous studies, TMP decreased NO production in human polymorphonuclear leukocytes and suppressed iNOS expression in rodent models of endotoxic shock (Wu et al., 1999; Zhang et al., 2003). Consistent with these results, we found that TMP pretreatment not only inhibited NO secretion, but suppressed iNOS protein level through the blockade of iNOS transcription in LPS-induced N9 cells. Incubation of N9 cells with TMP (25–100 μg/ml) for 24 h showed no significant cytotoxic effect on cell viability, implying that the down-regulation of NO and iNOS levels by TMP pretreatment was not due to a decrease in cell numbers. Because TMP displayed no direct scavenging effect on nitrite level in SNP solution, we supposed that TMP may inhibit LPS-induced NO production following by the suppression of iNOS in N9 cells. There have been still some contrary results regarding the effect of TMP on NO level. For instance, TMP can stimulate NO production in human platelets through activation of NOS (Sheu et al., 2000). These contradictory biological effects of TMP may depend, at least in part, on different cell types and changed oxidative status of cells.

NF-κB is an important transcription factor mainly involved in mediating inflammatory responses. Commonly, NF-κB is located in cytoplasm as an inactive complex bound to its inhibitory factor κB-α (IκB-α) (Rajan et al., 2008). Once activated by LPS, IL-1β or other inflammatory mediators, NF-κB is disassociated from IκB-α and translocates into nucleus to trigger the transcription of its target genes (Meng et al., 2008). It has been reported that the promoter region of murine gene encoding iNOS contains NF-κB binding site (Xie et al., 1994), and activation of NF-κB is proved to be a key component of NO and iNOS production in LPS-induced microglial cells (Kim et al., 2004). Indeed, this study revealed that, for NF-κB p65 level, LPS markedly led to a decrease in cytoplasm of N9 cells and an increase in nucleus, which was effectively reversed by TMP treatment. Studies by Hwang et al. (2004) showed that suppression

of NF-κB activity by its chemical inhibitor repressed IFN-γ-induced NO generation in microglial cells. Hence, it appears that nuclear inhibition of NF-κB activation by TMP is critical for suppression of NO and iNOS in N9 cells.

MAPKs are mainly composed of three well-characterized subfamilies including p38 MAPK, ERK1/2 and JNK, which elicit many cellular functions in physiology and pathological diseases (Johnson and Lapadat, 2002). It has been documented that MAPKs are upstream modulators for iNOS expression in microglial cells (Jung et al., 2009). In the case of LPS-induced NF-κB activation and subsequent NO and iNOS production, a pivotal role for three MAPK members in signaling transduction of microglial cells was identified (Ock et al., 2009). Thus, on the basis of our results that TMP inhibited LPS-induced NF-κB activation in N9 cells, we further investigated the suppressive effect of TMP on MAPK phosphorylation. We found that TMP pretreatment failed to influence the phosphorylation of p38 MAPK, ERK1/2 and JNK in vehicle-treated N9 cells (data not shown), but remarkably down-regulated the increase in phosphorylated levels of three MAPK members in LPS-induced N9 cells. Additionally, specific MAPK inhibitors, SB203580 against p38 MAPK, PD98059 against ERK1/2 and SP600125 against JNK, significantly suppressed the over-expression of iNOS protein in LPS-induced N9 cells, confirming the involvement of MAPKs in suppression of NO and iNOS by TMP. These results suggest that blockade of MAPK pathways may be a molecular mechanism underlying the inhibitory effect of TMP on NF-κB activation, and NO and iNOS production in microglial cells.

Paralleled by the MAPK signaling pathway, PI3K and its downstream signaling molecule, Akt, are also necessary regulators in the control of NF-κB activation and inflammatory cytokine synthesis in several cell types. The PI3K/Akt pathway, most frequently associated with regulation of cell growth and survival, was recently suggested to be positively correlated with LPS-induced iNOS expression in microglial cells (Kauffmann-Zeh et al., 1997; Oh et al., 2009). This was supported by the involvement of PI3K/Akt pathway in regulation of iNOS expression in manganese-induced microglial cells (Bae et al., 2006). In accordance with the above studies, our findings indicate that LPS stimulation induced evident increase in phosphorylated levels of both PI3K and Akt in N9 cells. Furthermore, the up-regulation of iNOS protein level by LPS challenge was reversed by specific PI3K inhibitor, LY294002, providing the direct evidence that PI3K/Akt pathway is implicated in the regulation of NO and iNOS production in microglial cells. Similarly, in the studies by Hwang et al. (2004) LY294002 blocked IFN-γ-induced iNOS mRNA expression and subsequent NO production in BV2 microglial cells. On the other hand, although TMP pretreatment had no effect on phosphorylated levels of both PI3K and Akt in vehicle-treated N9 cells (data not shown), it displayed evident inhibitory effect on Akt phosphorylation in LPS-induced N9 cells. Collectively, the inhibitory effect of TMP on NO and iNOS production in microglial cells might be partly contributed to the suppression of Akt activation. Regretfully, TMP failed to inhibit LPS-induced PI3K activation, so further studies should be performed to determine which signal molecule (s) led to the inhibition of Akt activation by TMP.

Intracellular ROS is a group of signaling molecules which mediated diverse cellular events such as inflammatory reactions (Kang et al., 2001). Over-production of ROS in microglial cells is strongly linked to brain injuries with high levels of inflammatory mediators including TNF-α, IL-1β and iNOS (Min et al., 2004). Based on these facts, the suppression of ROS may be an effective way to protect microglial cells from inflammatory damage. In previous investigations, TMP acted as an antioxidant that reduced angiotensin II-induced intracellular ROS production by interfering with the ERK1/2 pathway in vascular endothelial cells and smooth muscle cells (Lee et al., 2005; Zheng et al., 2006). In line with the above reports, our studies show that TMP pretreatment exerted inhibitory effect on LPS-induced ROS formation in N9 cells. We thus proposed that inhibition of NO and iNOS production in N9 cells may be attributed to the elimination of intracellular ROS by TMP. Studies by Koh et al. (2009) and by Oh et al. (2009) showed that ROS mainly acted as second messengers to amplify the inflammatory signals through activation of p38 MAPK, JNK and Akt in microglial cells. Therefore, ROS may act upstream of MAPKs and Akt or in separate pathways with crosstalk, and this remains to be determined.

Because of extensive fist-pass metabolism, TMP is recommended to be given intravenously instead of oral administration in the treatment (Qi et al., 2002). Considering the dose range of TMP (1–10 mg/kg) used in *in vivo* studies, efficient permeability to blood–brain barrier, and comparable protein binding in serum-supplemented media and plasm (Liang et al., 1999; Tan, 2009; Tsai and Liang, 2001), we consider that the concentrations of TMP used for cell culture experiments might be relevant to plasma and tissue levels achievable clinically.

In conclusion, our findings demonstrate that TMP inhibited LPS-induced over-production of NO and iNOS in N9 cells. The molecular regulation that directed protective effect of TMP may be performed through inhibition of NF-κB activation, blockade of MAPK and Akt phosphorylation, and suppression of intracellular ROS formation. In consideration of the potential cellular role and the novel signal transduction mechanisms for TMP in regulating microglial inflammation, our study shed light on the future application for TMP in treatment of neurodegenerative diseases.

## Acknowledgments

This work was supported by National Programs for High Technology Research and Development (863 Programs, 2006AA100313and 2007AA10Z343), and by Science Fund of Chongqing Medical University, China (XBZD200806).

## References

Bae, J.H., Jang, B.C., Suh, S.I., Ha, E., Baik, H.H., Kim, S.S., Lee, M.Y., Shin, D.H., 2006. Manganese induces inducible nitric oxide synthase (iNOS) expression via activation of both MAP kinase and PI3K/Akt pathways in BV2 microglial cells. Neuroscience Letters 398, 151–154.

Bal-Price, A., Brown, G.C., 2001. Inflammatory neurodegeneration mediated by nitric oxide from activated glia-inhibiting neuronal respiration, causing glutamate release and excitotoxicity. Journal of Neuroscience 21, 6480–6491.

Bamberger, M.E., Harris, M.E., McDonald, D.R., Husemann, J., Landreth, G.E., 2003. A cell surface receptor complex for fibrillar beta-amyloid mediates microglial activation. Journal of Neuroscience 23, 2665–2674.

Bhat, N.R., Fan, F., 2002. Adenovirus infection induces microglial activation: involvement of mitogen-activated protein kinase pathways. Brain Research 948, 93–101.

Bi, X.L., Yang, J.Y., Dong, Y.X., Wang, J.M., Cui, Y.H., Ikeshima, T., Zhao, Y.Q., Wu, C.F., 2005. Resveratrol inhibits nitric oxide and TNF-alpha production by lipopolysaccharide-activated microglia. International Immunopharmacology 5, 185–193.

Block, M.L., Zecca, L., Hong, J.S., 2007. Microglia-mediated neurotoxicity: uncovering the molecular mechanisms. Nature Reviews Neuroscience 8, 57–69.

Brochu, S., Olivier, M., Rivest, S., 1999. Neuronal activity and transcription of proinflammatory cytokines, IkappaBalpha, and iNOS in the mouse brain during acute endotoxemia and chronic infection with *Trypanosoma brucei*. Journal of Neuroscience Research 57, 801–816.

Chang, Y., Lee, J.J., Hsieh, C.Y., Hsiao, G., Chou, D.S., Sheu, J.R., 2009. Inhibitory effects of ketamine on lipopolysaccharide-induced microglial activation. Mediators of Inflammation 2009, 705379.

Fu, Y.S., Lin, Y.Y., Chou, S.C., Tsai, T.H., Kao, L.S., Hsu, S.Y., Cheng, F.C., Shih, Y.H., Cheng, H., Fu, Y.Y., Wang, J.Y., 2008. Tetramethylpyrazine inhibits activities of glioma cells and glutamate neuro-excitotoxicity: potential therapeutic application for treatment of gliomas. Neuro-Oncology 10, 139–152.

Garrido, G., Delgado, R., Lemus, Y., Rodríguez, J., García, D., Núñez-Sellés, A.J., 2004. Protection against septic shock and suppression of tumor necrosis factor alpha and nitric oxide production on macrophages and microglia by a standard aqueous extract of *Mangifera indica* L. (VIMANG). Pharmacological Research 50, 165–172.

Hwang, S.Y., Jung, J.S., Lim, S.J., Kim, J.Y., Kim, T.H., Cho, K.H., Han, I.O., 2004. LY294002 inhibits interferon-gamma-stimulated inducible nitric oxide syn-

thase expression in BV2 microglial cells. Biochemical and Biophysical Research Communications 318, 691–697.
Inoue, K., 2002. Microglial activation by purines and pyrimidines. Glia 40, 156–163.
Johnson, G.L., Lapadat, R., 2002. Mitogen-activated protein kinase pathways mediated by ERK, JNK, and p38 protein kinases. Science 298, 1911–1912.
Jung, H.W., Yoon, C.H., Park, K.M., Han, H.S., Park, Y.K., 2009. Hexane fraction of Zingiberis Rhizoma Crudus extract inhibits the production of nitric oxide and proinflammatory cytokines in LPS-stimulated BV2 microglial cells via the NF-kappaB pathway. Food and Chemical Toxicology 47, 1190–1197.
Kang, J., Park, E.J., Jou, I., Kim, J.H., Joe, E.H., 2001. Reactive oxygen species mediate A beta(25–35)-induced activation of BV-2 microglia. Neuroreport 12, 1449–1452.
Kao, T.K., Ou, Y.C., Kuo, J.S., Chen, W.Y., Liao, S.L., Wu, C.W., Chen, C.J., Ling, N.N., Zhang, Y.H., Peng, W.H., 2006. Neuroprotection by tetramethylpyrazine against ischemic brain injury in rats. Neurochemistry International 48, 166–176.
Kauffmann-Zeh, A., Rodriguez-Viciana, P., Ulrich, E., Gilbert, C., Coffer, P., Downward, J., Evan, G., 1997. Suppression of c-Myc-induced apoptosis by Ras signalling through PI(3)K and PKB. Nature 385, 544–548.
Kilic, B., Kruse, M., Stahlmann, R., 2006. The in vitro effects of quinupristin/dalfopristin, erythromycin and levofloxacin at low concentrations on the expression of different cell adhesion molecules on the surface of endothelial cells (Eahy926). Toxicology 218, 30–38.
Kim, W.K., Hwang, S.Y., Oh, E.S., Piao, H.Z., Kim, K.W., Han, I.O., 2004. TGF-beta1 represses activation and resultant death of microglia via inhibition of phosphatidylinositol 3-kinase activity. Journal of Immunology 172, 7015–7023.
Koh, K., Cha, Y., Kim, S., Kim, J., 2009. tBHQ inhibits LPS-induced microglial activation via Nrf2-mediated suppression of p38 phosphorylation. Biochemical and Biophysical Research Communications 380, 449–453.
Lee, W.S., Yang, H.Y., Kao, P.F., Liu, J.C., Chen, C.H., Cheng, T.H., Chan, P., 2005. Tetramethylpyrazine downregulates angiotensin II-induced endothelin-1 gene expression in vascular endothelial cells. Clinical and Experimental Pharmacology and Physiology 32, 845–850.
Liang, C.C., Hong, C.Y., Chen, C.F., Tsai, T.H., 1999. Measurement and pharmacokinetic study of tetramethylpyrazine in rat blood and its regional brain tissue by high-performance liquid chromatography. Journal of Chromatography B: Biomedical Sciences and Application 724, 303–309.
Liu, C.F., Lin, M.H., Lin, C.C., Chang, H.W., Lin, S.C., 2002. Protective effect of tetramethylpyrazine on absolute ethanol-induced renal toxicity in mice. Journal of Biomedical Science 9, 299–302.
Ma, J., Hwang, Y.K., Cho, W.H., Han, S.H., Hwang, J.K., Han, J.S., 2009. Macelignan attenuates activations of mitogen-activated protein kinases and nuclear factor kappa B induced by lipopolysaccharide in microglial cells. Biological & Pharmaceutical Bulletin 32, 1085–1090.
Marcocci, L., Maguire, J.J., Droy-Lefaix, M.T., Packer, L., 1994. The nitric oxide-scavenging properties of Ginkgo biloba extract EGb 761. Biochemical and Biophysical Research Communications 201, 748–755.
Meng, X.L., Yang, J.Y., Chen, G.L., Zhang, L.J., Wang, L.H., Li, J., Wang, J.M., Wu, C.F., 2008. RV09, a novel resveratrol analogue, inhibits NO and TNF-alpha production by LPS-activated microglia. International Immunopharmacology 8, 1074–1082.
Min, K.J., Pyo, H.K., Yang, M.S., Ji, K.A., Jou, I., Joe, E.H., 2004. Gangliosides activate microglia via protein kinase C and NADPH oxidase. Glia 48, 197–206.
Moncada, S., Palmer, R.M., Higgs, E.A., 1991. Nitric oxide: physiology, pathophysiology, and pharmacology. Pharmacological Reviews 43, 109–142.
Mukaida, N., Ishikawa, Y., Ikeda, N., Fujioka, N., Watanabe, S., Kuno, K., Matsushima, K., 1996. Novel insight into molecular mechanism of endotoxin shock: biochemical analysis of LPS receptor signaling in a cell-free system targeting NF-kappaB and regulation of cytokine production/action through beta2 integrin in vivo. Journal of Leukocyte Biology 59, 145–151.
Nizamutdinova, I.T., Jeong, J.J., Xu, G.H., Lee, S.H., Kang, S.S., Kim, Y.S., Chang, K.C., Kim, H.J., 2008. Hesperidin, hesperidin methyl chalone and phellopterin from Poncirus trifoliata (Rutaceae) differentially regulate the expression of adhesion molecules in tumor necrosis factor-alpha-stimulated human umbilical vein endothelial cells. International Immunopharmacology 8, 670–678.
Ock, J., Kim, S., Suk, K., 2009. Anti-inflammatory effects of a fluorovinyloxyacetamide compound KT-15087 in microglia cells. Pharmacological Research 59, 414–422.
Oh, Y.T., Lee, J.Y., Lee, J., Kim, H., Yoon, K.S., Choe, W., Kang, I., 2009. Oleic acid reduces lipopolysaccharide-induced expression of iNOS and COX-2 in BV2 murine microglial cells: possible involvement of reactive oxygen species, p38 MAPK, and IKK/NF-kappaB signaling pathways. Neuroscience Letters 464, 93–97.
Pawate, S., Shen, Q., Fan, F., Bhat, N.R., 2004. Redox regulation of glial inflammatory response to lipopolysaccharide and interferongamma. Journal of Neuroscience Research 77, 540–551.
Qi, X., Ackermann, C., Sun, D., Liu, R., Sheng, M., Hou, H., 2002. The prediction of plasma and brain levels of 2,3,5,6-tetramethylpyrazine following transdermal application. AAPS PharmSci. 4, E46.
Qin, L., Liu, Y., Wang, T., Wei, S.J., Block, M.L., Wilson, B., Liu, B., Hong, J.S., 2004. NADPH oxidase mediates lipopolysaccharide-induced neurotoxicity and proinflammatory gene expression in activated microglia. Journal of Biological Chemistry 279, 1415–1421.
Rajan, S., Ye, J., Bai, S., Huang, F., Guo, Y.L., 2008. NF-kappaB, but not p38 MAP kinase, is required for TNF-alpha-induced expression of cell adhesion molecules in endothelial cells. Journal of Cellular Biochemistry 105, 477–486.
Sheu, J.R., Kan, Y.C., Hung, W.C., Lin, C.H., Yen, M.H., 2000. The antiplatelet activity of tetramethylpyrazine is mediated through activation of NO synthase. Life Science 67, 937–947.
So, E.C., Wong, K.L., Huang, T.C., Tasi, S.C., Liu, C.F., 2002. Tetramethylpyrazine protects mice against thioacetamide-induced acute hepatotoxicity. Journal of Biomedical Science 9, 410–414.
Stoll, G., Jander, S., 1999. The role of microglia and macrophages in the pathophysiology of the CNS. Progress in Neurobiology 58, 233–247.
Tan, Z., 2009. Neural protection by naturopathic compounds—an example of tetramethylpyrazine from retina to brain. Journal of Ocular Biology, Diseases, and Informatics 2, 57–64.
Tarozzi, A., Morroni, F., Hrelia, S., Angeloni, C., Marchesi, A., Cantelli-Forti, G., Hrelia, P., 2007. Neuroprotective effects of anthocyanins and their in vivo metabolites in SH-SY5Y cells. Neuroscience Letter 424, 36–40.
Tsai, T.H., Liang, C., 2001. Pharmacokinetics of tetramethylpyrazine in rat blood and brain using microdialysis. International Journal of Pharmaceutics 216, 61–66.
Wang, B., Navath, R.S., Romero, R., Kannan, S., Kannan, R., 2009. Anti-inflammatory and anti-oxidant activity of anionic dendrimer-N-acetyl cysteine conjugates in activated microglial cells. International Journal of Pharmaceutics 377, 159–168.
Wu, C.C., Liao, M.H., Chen, S.J., Yen, M.H., 1999. Tetramethylpyradizine prevents inducible NO synthase expression and improves survival in rodent models of endotoxic shock. Naunyn-Schmiedeberg's Archives of Pharmacology 360, 435–444.
Xie, Q.W., Kashiwabara, Y., Nathan, C., 1994. Role of transcription factor NF-kappa B/Rel in induction of nitric oxide synthase. Journal of Biological Chemistry 269, 4705–4708.
Xu, S.Z., Zhong, W., Watson, N.M., Dickerson, E., Wake, J.D., Lindow, S.W., Newton, C.J., Atkin, S.L., 2008. Fluvastatin reduces oxidative damage in human vascular endothelial cells by upregulating Bcl-2. Journal of Thrombosis and Haemostasis 6, 692–700.
Zhang, Z., Wei, T., Hou, J., Li, G., Yu, S., Xin, W., 2003. Tetramethylpyrazine scavenges superoxide anion and decreases nitric oxide production in human polymorphonuclear leukocytes. Life Science 72, 2465–2472.
Zheng, H., Chen, X.L., Han, Z.X., Wang, S.Y., Chen, Z.W., 2006. Effect of Ligustrazine on liver injury after burn trauma. Burns 32, 328–334.
Zhou, Y., Hu, C.P., Deng, P.Y., Deng, H.W., Li, Y.J., 2004. The protective effects of ligustrazine on schemia-reperfusion and DPPH free radical-induced myocardial injury in isolated rat hearts. Planta Med. 70, 818–822.
Zhu, Y.M., Azahri, N.S., Yu, D.C., Woll, P.J., 2008. Effects of COX-2 inhibition on expression of vascular endothelial growth factor and interleukin-8 in lung cancer cells. BMC Cancer 8, 218.